



Since January 2020 Elsevier has created a COVID-19 resource centre with free information in English and Mandarin on the novel coronavirus COVID-19. The COVID-19 resource centre is hosted on Elsevier Connect, the company's public news and information website.

Elsevier hereby grants permission to make all its COVID-19-related research that is available on the COVID-19 resource centre - including this research content - immediately available in PubMed Central and other publicly funded repositories, such as the WHO COVID database with rights for unrestricted research re-use and analyses in any form or by any means with acknowledgement of the original source. These permissions are granted for free by Elsevier for as long as the COVID-19 resource centre remains active.



Experimental study of the purification performance of a MopFan-based photocatalytic air cleaning system

Emmanuel Tapia-Brito^{a,*}, James Riffat^a, Yixin Wang^a, Yuhao Wang^a, Amir M. Ghaemmaghami^b, Christopher M. Coleman^c, Mehmet T. Erdinç^d, Saffa Riffat^a

^a Department of Architecture and Built Environment, University of Nottingham, University Park, Nottingham, NG7 2RD, UK

^b Immunology & Immuno-bioengineering Group, School of Life Sciences, University of Nottingham, University Park, Nottingham, NG7 2RD, UK

^c School of Life Sciences, University of Nottingham, Queen's Medical Centre, Nottingham, NG7 2UH, UK

^d Department of Mechanical Engineering, Tarsus University, Tarsus, Mersin, 33400, Turkey

ARTICLE INFO

Keywords:

Air purification
Air cleaning device
Photocatalysis
Photocatalytic oxidation

ABSTRACT

Severe acute respiratory syndrome coronavirus (SARS-CoV)-2, the virus that causes the coronavirus disease (COVID)-19, is primarily transmitted through respiratory droplets which linger in enclosed spaces, often exacerbated by HVAC systems. Although research to improve HVAC handling of SARS-CoV-2 is progressing, currently installed HVAC systems cause problems because they recirculate air and use ineffective filters against virus. This paper details the process of developing a novel method of eliminating air pollutants and suspended pathogens in enclosed spaces using Photocatalytic Oxidation (PCO) technology. It has been previously employed to remove organic contaminants and compounds from air streams using the irradiation of titanium dioxide (TiO₂) surfaces with ultraviolet (UV) lights causing the disintegration of organic compounds by reactions with oxygen (O) and hydroxyl radicals (OH). The outcome was two functional prototypes that demonstrate the operation of PCO-based air purification principle. These prototypes comprise a novel TiO₂ coated fibre mop system, which provide very large surface area for UV irradiation. Four commercially accessible materials were used for the construction of the mop: Tampico, Brass, Coco, and Natural synthetic. Two types of UV lights were used: 365 nm (UVA) and 270 nm (UVC). A series of tests were conducted that proved the prototype's functionality and its efficiency in lowering volatile organic compounds (VOCs) and formaldehyde (HCHO). The results shown that a MopFan with rotary mop constructed with Coco fibres and utilising UVC light achieves the best VOC and HCHO purification performance. Within 2 h, this combination lowered HCHO by 50% and VOCs by 23% approximately.

1. Introduction

As a result of the COVID-19 pandemic, people became increasingly concerned about the air quality in their homes, places of business, and public spaces. The elimination of any other suspended pollutant that may provide a risk to human health needs continued research into air purification, not only regarding infectious diseases, but also to remove any other suspended pollutants that may pose a risk to human health. Approximately 3.8 million deaths were related to indoor air pollution in 2017 globally. (IAP). IAP raises the chance of developing lung cancer, heart disease, COPD, and stroke. The average British citizen spends 90% of his or her life indoors [1]. As a result, there is a growing emphasis on achieving clean air for breathing. The Clean Air Bill is being debated in the UK parliament, and its objective is to establish that breathing clean

air is a fundamental human right. The Environment Act, an aim set by the UK Environment Agency for 2030 to prevent the deterioration of nature and specifically reduce ambient PM 2.5 concentrations, the most hazardous pollutant to human health, demonstrates this further. Air purifiers and other portable IAQ devices vary in design and function. Photocatalytic air purifiers are distinct from those that utilise a high efficiency particulate arrestment (HEPA) filter. Traditional air purifiers transmit airborne particles to a filter. These filters must be replaced for the purifier to operate correctly. The time intervals between replacements will vary based on the purifier's usage and climate. However, photocatalytic purifiers are capable of deactivating viruses, particulates, and other contaminants without leaving any trace on the filter surface. At room temperature, photocatalytic oxidation (PCO) may degrade numerous pollutants into CO₂ and H₂O, rendering them

* Corresponding author.

E-mail address: b_tapi@hotmail.com (E. Tapia-Brito).

<https://doi.org/10.1016/j.buildenv.2023.110422>

Received 5 March 2023; Received in revised form 29 April 2023; Accepted 15 May 2023

Available online 16 May 2023

0360-1323/© 2023 The Authors. Published by Elsevier Ltd. This is an open access article under the CC BY license (<http://creativecommons.org/licenses/by/4.0/>).

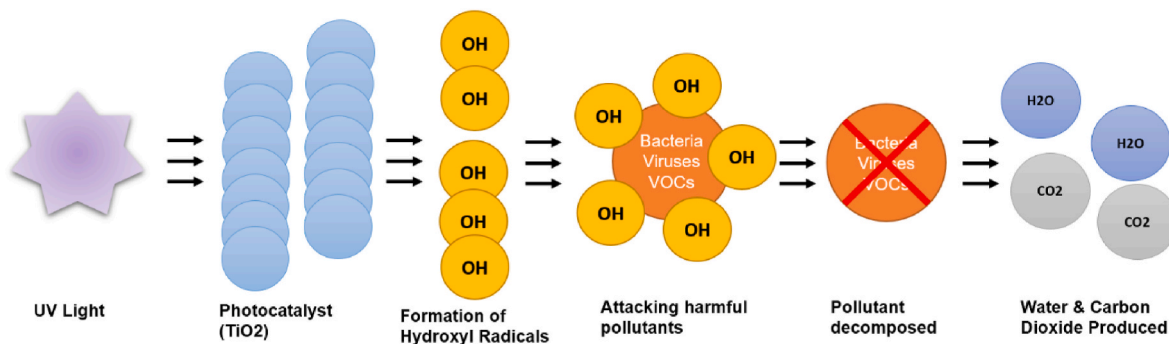


Fig. 1. Photocatalytic oxidation.

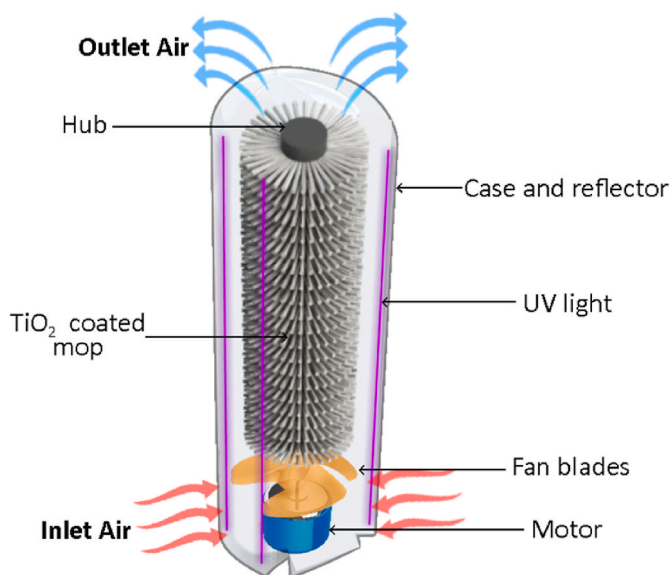


Fig. 2. MopFan concept diagram.

harmless to inhabitants. These toxins include formaldehyde (HCHO), toluene, PM2.5 and other volatile organic compounds (VOCs). The use of PCO in air purifiers has application potential in business and residential buildings, the aerospace industry, and automobiles.

1.1. Background of air purification devices

In the context of air purification devices, various technologies have emerged, each demonstrating distinct characteristics and mechanisms for purifying indoor air.

High-efficiency particulate air (HEPA) purifiers utilise a specific type of filter, known as a HEPA filter, which is designed to remove at least 99.97% of particulates with a diameter of 0.3 μm. The effectiveness of HEPA purifiers often depends on factors such as room size, usage, occupant number, filter size, and air circulation efficiency. These purifiers typically employ a fan system to circulate air through the filter before releasing it back into the room.

Adsorbent purifiers, in contrast, rely on adsorbent materials, which can attract pollutants to their surface via chemical or physical processes. These purifiers can be constructed from eco-friendly materials and plant extractions, with activated carbon being a common example of an adsorbent material used for the removal of CO₂, NO₂, and SO₂.

Ultraviolet (UV) purifiers employ a UV lamp emitting UV-C light to expose the air to ultraviolet germicidal irradiation (UVGI). This process breaks chemical bonds in DNA molecules, effectively inactivating viruses and eliminating fungi and bacteria. The prevalence of UV purifiers has increased significantly over the past decade, with various purification methods available.

Ionic purifiers generate ions that are either positively or negatively charged. These devices often produce negative ions through a process called corona discharge, which causes particulate matter to attach to ions and settle on surfaces, where they can be cleaned. The performance of negative air ionisers (NAIs) is influenced by factors such as turbulence intensity and dielectric constraints of particles, which affect their deposition and electric mobility.

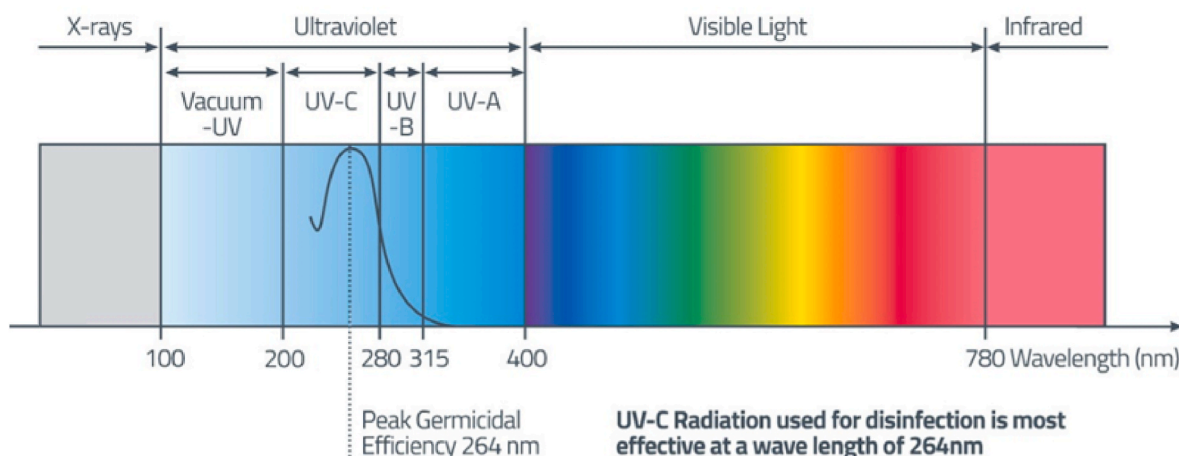
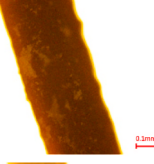


Fig. 3. The light spectrum and UV wavelength ranges.

Table 1
Micrographic comparison of the coated bristles.

Material	TiO ₂ solution (no SA)	TiO ₂ solution (with SA)	Observations
Crimpled brass			Without SA, the solution begins to flake out from the sample. The underlying material's reflections are visible, thus it is not totally covered by the solution. In the sample with SA, the base material cannot be seen. The surface of the bristle exhibits irregularities (lumps).
Natural synthetic			The plastic material is translucent. In the sample without SA, it allows the passage of light, revealing that the coating did not cling to the full bristle surface. In the sample with SA, a uniform layer of solution is obtained. The cover in this instance formed few lumps.
Organic Coco			This material is dark. The darker areas in the sample without SA suggest that the coverage there is thin. The lighter areas are lumps. In the sample with SA, a smooth, homogenous layer is observed.
Organic Tampico			This material is light in color. In the sample without SA, despite the solution adhering uniformly, a thin layer is noticed. Presumably, the material absorbs some of the covering. The sample with SA is noticeably darker, indicating a thicker cover layer. There are relatively few imperfections on the surface.
Crimpled steel			In the sample without SA, the base material's striations are visible, indicating that the covering is extremely thin and not uniform. The coverage in the sample with SA, although is thicker, is not uniform either. However, adhesion is better.
Hand-sanded plastic			Due to the fact that this material is sanded by hand, the bristles' surface and thickness are uneven. The SA sample is not homogenous, exposing places with more coverage than others. The sample with SA exhibits the same homogeneity issue, although to a lesser degree.
Pre sanded plastic			This material is sanded by a machine, so its diameter stays consistent. The surface irregularities of pre-sanded bristle are fewer than those of hand-sanded bristle. In this case both samples are very similar. However, the sample with SA shows a thicker layer of cover.

Electrostatic precipitators (ESPs) function by utilising positively charged plates to attract particulate matter. These devices have gained popularity over ionisers, as they collect particles on plates rather than dispersing them throughout a room, simplifying the cleaning process. ESPs can operate either as in-duct or standalone units, offering silent operation and considerable benefits to users.

1.2. Photocatalytic oxidation devices

Photocatalytic oxidation (PCO) occurs when pollutants react with a semiconducting material such as Titanium Dioxide (TiO₂). This is the most used photocatalyst because it may be used at room temperature, is safe and inexpensive, effectively destroys a variety of contaminants, and requires no additional chemical additions. The UV light illuminates this catalyst. The wavelength can range between 180 nm and 400 nm. As seen in Fig. 1, this produces hydroxyl radicals and oxide ions that attract and oxidise contaminants. In theory, the contaminants are then broken down into water vapour and carbon dioxide. Purifiers with PCO function

have an advantage since the pollutants begin to disintegrate into non-hazardous components during the PCO reaction, whereas HEPA filters may still contain harmful pollutants on the filter surface [2].

In the last two decades, UV-PCO technology has become increasingly prevalent. The application of this technique for interior air cleaning has attracted considerable interest. There are various by-products that can be produced by the PCO reaction, and investigations have been carried out to determine their concentration [3]. A new vacuum ultraviolet oxidation (VUV-PCO) air purifier was tested in China. The purifier had a nanoporous TiO₂ film, a radial fan, and a Mn-Fe catalyst. This purifier's elimination of VOCs and O₃ was investigated. These tests were conducted in an airtight chamber. The results revealed that the purifier reduced formaldehyde, nonanal, pentanal, benzene, toluene, octanal, o,m-xylene, and ortho-xylene by up to 78.71%. The purifier was also fitted with a heated ozone removal device that assisted in the removal of volatile organic compounds. This study highlights the potential of VUC-PCO air purifiers and the necessity for additional exploration in situations with greater diversity [4].

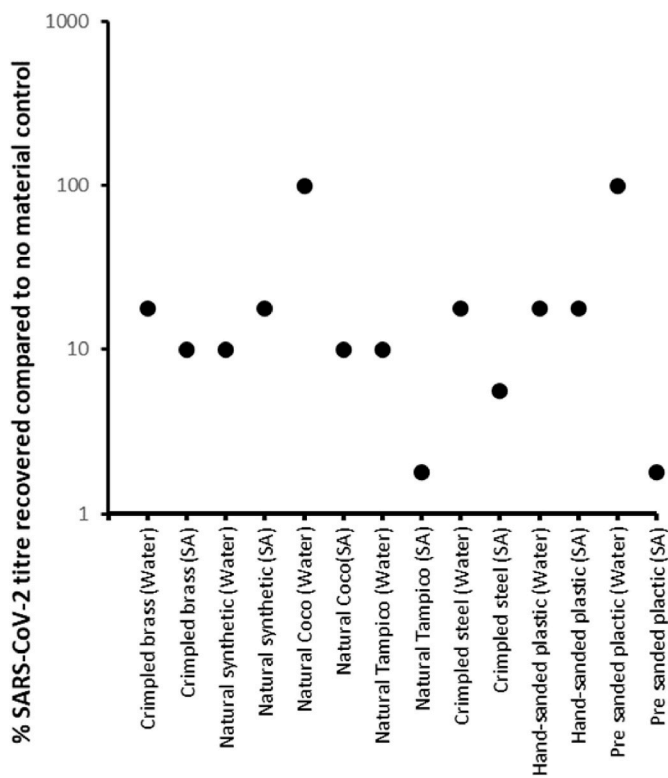


Fig. 4. Antiviral activity of materials. Each surface was tested once.

A study conducted in France examined the effectiveness of various photocatalytic air purifiers that are commercially available. The study indicated that the design and installation of a PCO air purifier are crucial components. Despite operating at a lower flow rate, while comparing the purifiers, certain purifiers functioned more efficiently than others due to the photocatalytic substance being better distributed to the source of irradiation and an optimised assembly of the lamp/photocatalyst and/or fan. In other research, TiO₂-coated fibres instead of a coated metal plate have been utilised to analyse the PCO catalyst's layout. In a related investigation, the impacts of a large surface area of TiO₂ nanofibers were discovered to boost the adsorption capacity and visible light absorption. The TiO₂ nanofibers evaluated in this work are a promising choice for incorporation in air quality devices with enhanced air purification

efficiency and reduced energy demand [5]. In the study [6], a variety of PCO substrates were analysed. Increased surface area benefits the PCO reaction by allowing more oxygen and UV light to interact with the catalyst. Substrates like aluminium honeycomb mesh can provide a very large surface area without affecting the structural integrity of the filter. Due to the huge surface area, this might also result in a decrease in pressure, which increases the amount of energy required to utilise this as a filter. Also investigated were carbon fabric, nickel foam, and fibre-glass. As a filter, these substrates need less energy but have a smaller surface area. However, the most energy-intensive component of a photocatalytic purifier is its lights.

In a real-world smoking room, a study examined the efficiency of a TiO₂ type purifier, known for its effectiveness in reducing high levels of pollutants, particularly VOCs, found in tobacco smoke [7]. The catalyst employed was an MnO_x/TiO₂ coated filter. After a 30-min treatment period, the study reported a reduction in VOC concentration to 171 µg/m³ and decomposition of another pollutant, acetaldehyde. These results highlight the significant efficacy of this purifier in removing common airborne pollutants in real-world settings, with the MnO_x and TiO₂ catalyst performing well in both experimental setups and actual smoking rooms.

A study analysing the correlation of light-emitting diodes discovered numerous advantages, such as long life, low-temperature bulbs, and low pollution levels [8]. The illumination of the catalyst in specific UV light frequencies is crucial for the PCO reaction. The study found that a TiO₂ coated HEPA filter blocked the aerosol and that the concentration of *Staphylococcus aureus* decreased gradually upon exposure to UV light and the catalyst. After 52 h, all *Staphylococcus aureus* was eliminated, with the UV LED light performing better than a mercury lamp, demonstrating the feasibility of UV LED/TiO₂ for the PCO reaction.

A study by Ref. [9] investigated the use of a PCO purifier in a simulated aircraft cabin, where 17 subjects were exposed for 7 h. Chemical analysis indicated that the PCO units decomposed toluene, isoprene, and ethanol within the cabin. However, pollutants such as formaldehyde and acetaldehyde remained present. Although humidity levels stayed consistent, air conditions causing dizziness were observed. While the purifier effectively removed airborne pollutants, the negative impacts on air quality and occupant health raised concerns about the use of PCO purifiers in this setting.

In a study by Ref. [10]; a titania-zeolite composite bead filter was tested for its effectiveness in removing VOCs and viruses. It was found that the use of titania-zeolite enhanced photocatalytic activity, resulting in increased degradation of VOCs. The conversion of VOCs to CO₂ improved, and the adsorption capacity was superior. Tests on the

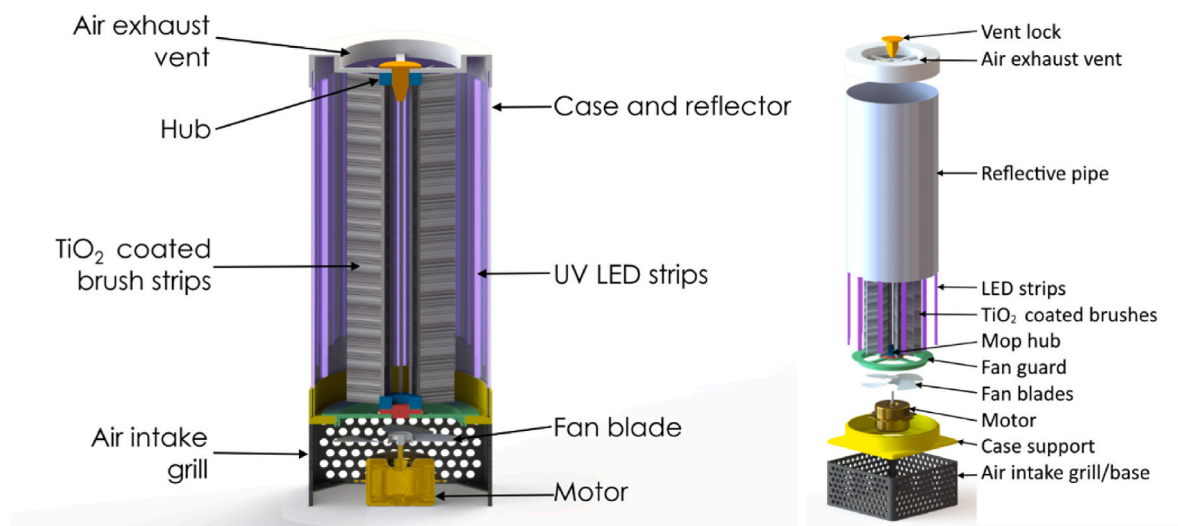


Fig. 5. Prototype CAD assembly: cross-section (left), exploded view (right).

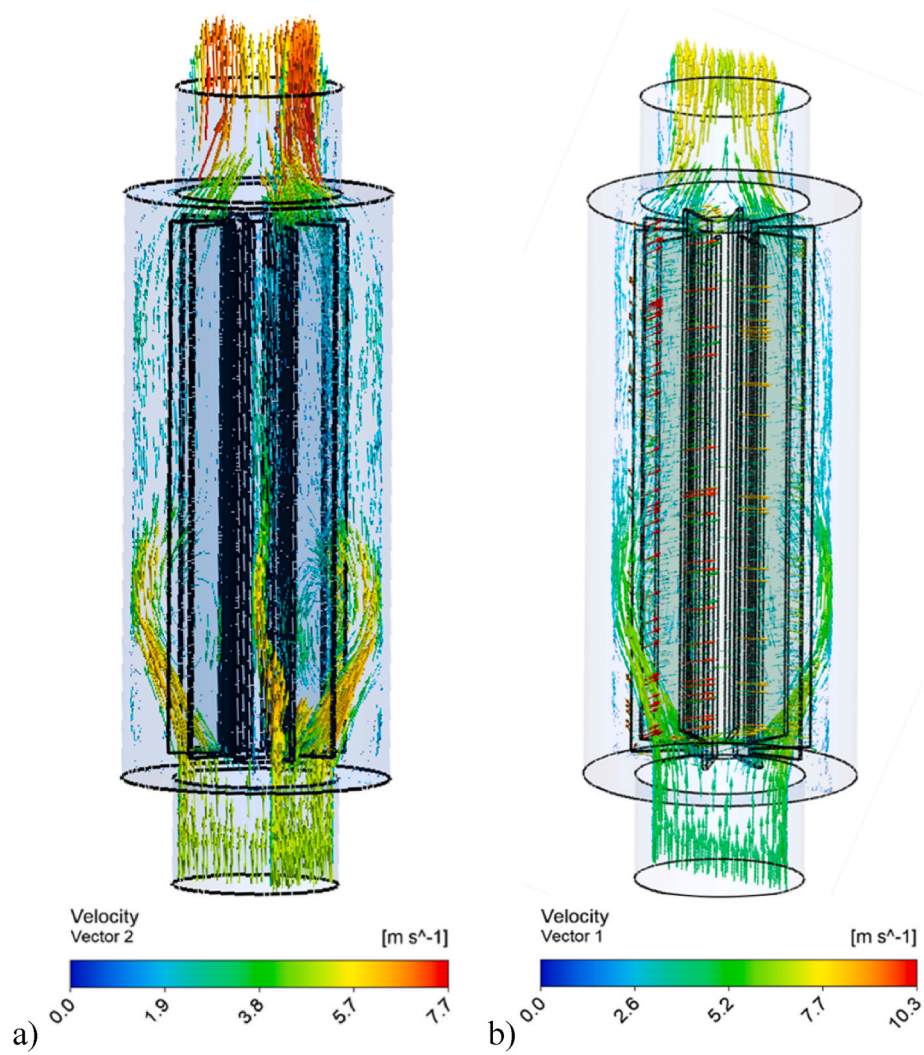


Fig. 6. Comparison of flow simulations a) Stationary mop, b) Rotating mop.

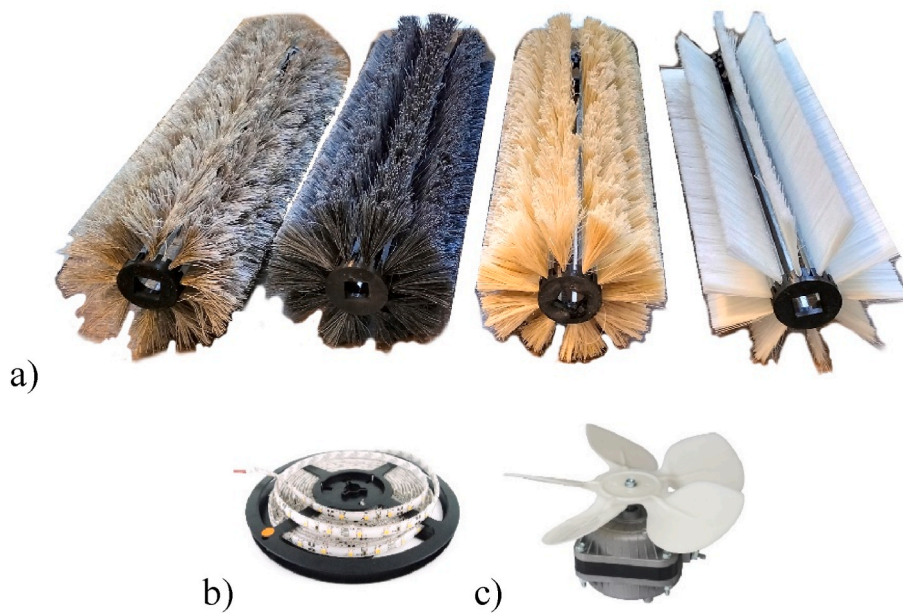


Fig. 7. Prototypes main components: a) Roller brushes constructed, b) UV LED strip, c) Motor with plastic fan blades.



Fig. 8. Prototypes constructed: “A” (left) and “B” (right).

regeneration and durability of this filter were also conducted. Bacteriophage Phi-X 174 was completely inactivated by the PCO reaction, and SARS-CoV-2 was inactivated within 1 h of treatment. The study concluded that this type of filter has practical applications and could be utilised in hospitals and homes.

[11] conducted a study in which a school gym was monitored for airborne pollutant concentrations. A portable air purifier was tested, and the concentration of indoor airborne pollutants was compared with outdoor pollutant concentrations and indoor concentrations before the purifier was activated. The study found significant reductions in indoor pollutant levels compared to outdoor pollutants, with air changes per hour increasing. Reductions as high as 70% and 84% were observed. Efficiency improvements were more noticeable when the test was performed in a smaller gym, likely due to the sizing of the purifier and room setting, with a larger purifier needed to achieve similar performance levels as in the smaller gym.

Another study examining the efficiency of mobile air purifiers was conducted by Ref. [12]. The study modelled indoor pollutant reduction using mobile purifiers in an exemplary lecture hall. Employing CFD modelling, the results varied depending on the location and orientation of the purifier within the lecture hall. With air changes per hour of 5, PM1 at average head height was reduced by as much as 75%. By calculating particle paths and airflow, the study found that steady simulation results correlated well with experimental findings, further demonstrating the efficiency of mobile purifiers for use within indoor settings.

Despite the encouraging results obtained in these studies, a research gap was identified, suggesting that the geometry of the filters utilised could be further optimised. In this regard, this study proposed that a brush-like structure be employed to enhance the air purification process. By adopting this innovative configuration, each fibre within the filter could be coated with TiO₂, thus maximising the available surface area for photocatalysis to occur.

Through the incorporation of this novel brush-like structure, it is anticipated that the overall effectiveness of the air purifiers examined in the previous studies would be significantly improved. Moreover, optimised filter geometry can contribute to reduced energy consumption in air purification systems. By maximising the contact area between the air

and the photocatalytic surface, the efficiency of the pollutant degradation process can be increased. This improvement allows for the utilisation of lower-powered systems or reduced operation times, leading to energy savings and lower operating costs. In the following section, a detailed explanation of the proposed brush-like structure will be provided, offering further insight into the potential benefits and advancements in filter design.

In [13], we provided a general overview of how the MopFan concept may be implemented in an air purifier device, focusing mainly on the design. This new article, on the other hand, proposes an improved version of the MopFan design for household usage.

The main objective of this paper is to present a set of laboratory trials in order to find the optimal MopFan configuration. For this purpose, a comprehensive analysis of the bristles' constituent materials has been conducted. An investigation on the air purifying and antiviral capabilities of such materials is also presented. In addition, the purifying performance of the MopFan with a static brush against the MopFan with a spinning brush is compared.

2. Description of the “MopFan” system

The system comprises of a cylindrical mop that resembles a chimney sweep brush but is constructed with flexible bristles coated with TiO₂. TiO₂-covered bristles organised in a mop arrangement offer an extraordinarily large UV-TiO₂ interaction surface area and airflow passage compared to typical filter/mesh UV systems.

This system was nicknamed MopFan because, on the one hand, it consists of the previously described cylindrical brush and, on the other, of a fan that pushes air through the brush's bristles until it comes out. The system's main components are illustrated in Fig. 2.

When the motor turns, the blades move along with it, pushing air from the outside upwards and into the bristles of the mop, which are also moving with the fan. UV light would act on the TiO₂ and initiate the photocatalytic reaction as contaminated air passes through the purifier's body. Simultaneously, the mop fan would push the filtered air to the device case's top air exit.

During operation, the air blown by the mop fan will traverse the vast surface area of the TiO₂ bristles. UV LEDs of high intensity are positioned within the fan housing to illuminate the broom. The interior surface of the housing is coated with a light-reflective substance in order to maximise UV ray concentration. The product is a fan system that provides excellent airflow and exceptionally high UV irradiation of TiO₂, producing a huge number of hydroxyl radicals to eliminate airborne pollutants such as VOCs, Formaldehyde, Chloride, Benzoin, Isobutane, Particulates, Dust, Allergens, etc.

This arrangement has been proved to be effective as an air impeller, attaining 97% of the performance of backward-curved centrifugal fans [14]. Since this first study, which created the mop-fan concept, UV LED and TiO₂ coating processes must undergo significant advancements.

The main reason for utilising a mop as a filter, is to increase the surface area where the photocatalytic reaction happens. Rather than having a flat surface where the reaction occurs, there is a much greater area in a mop filter, as the reaction occurs on the surface of each fibre. The mop inhibits the air from moving in a laminar flow and causes it to remain stuck between the fibres for longer, which favours its purification.

Because of its simple structure that does not require a large number of components, the system is reasonably inexpensive. TiO₂ has various commercial applications, thus it is not expensive or difficult to acquire. The materials selected for the mop fibres are commonly used in brushes for diverse functions. LED lighting is a technology whose price decreases continuously.

Flexibility is another benefit of the MopFan; this system can be scaled up to cleanse large volumes of air or reduced to a compact model.

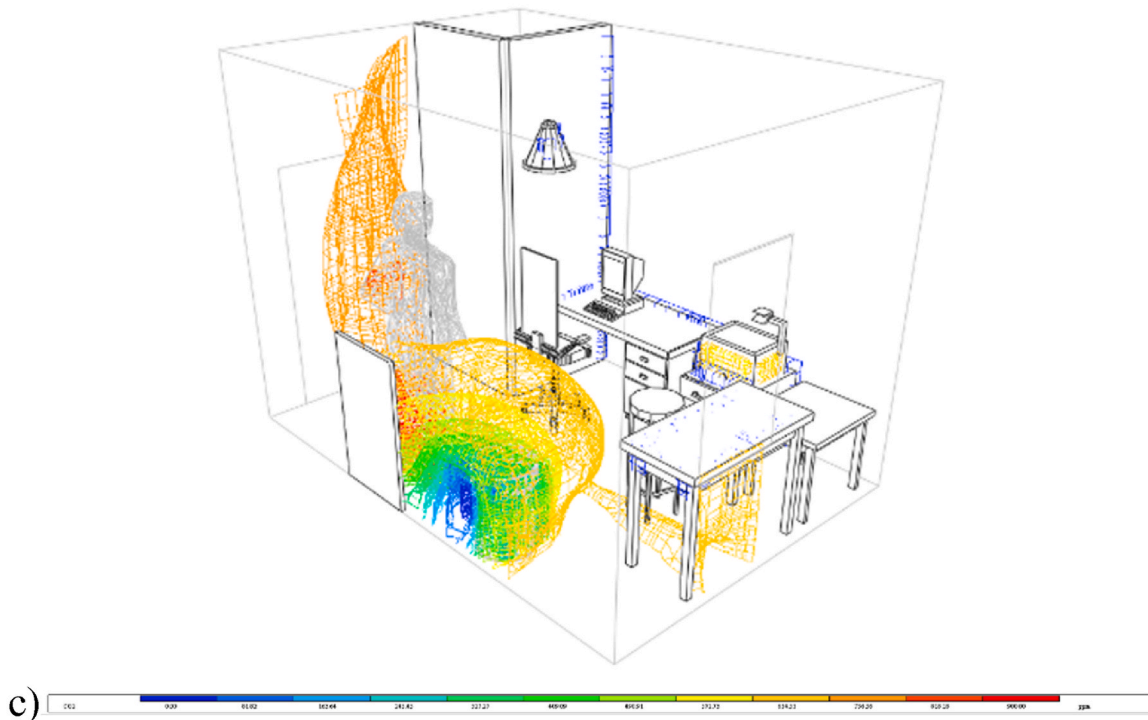
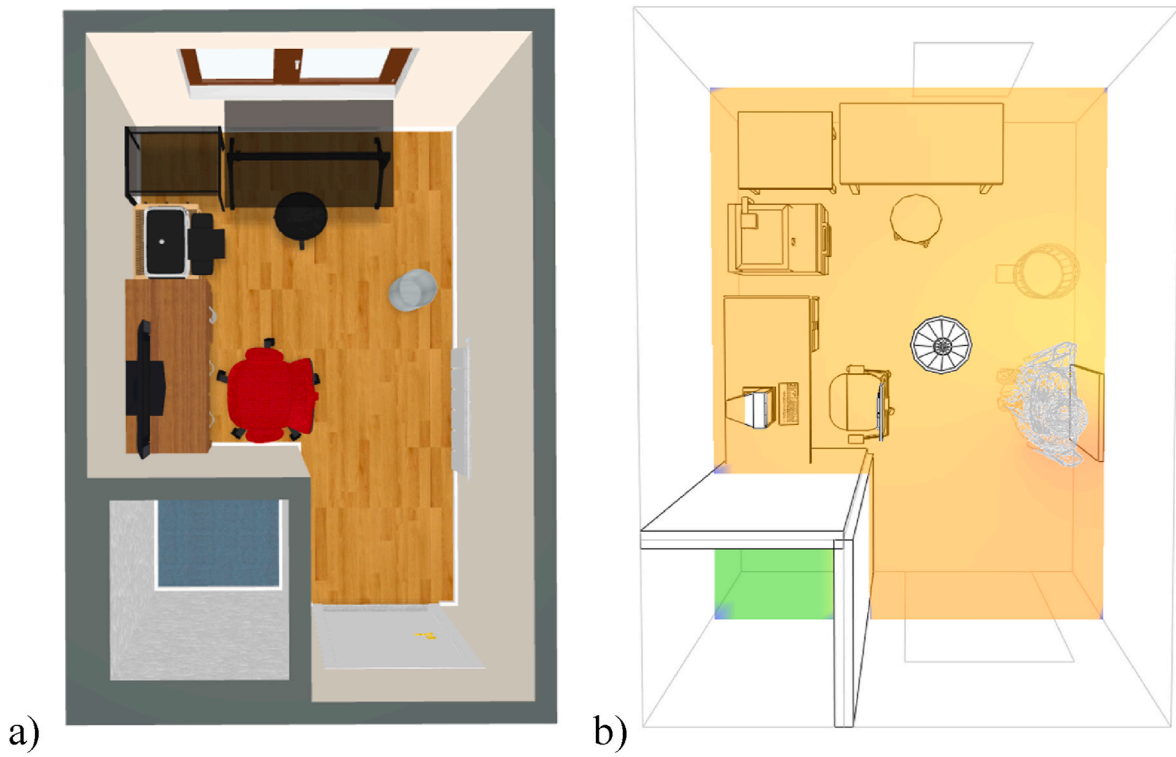




Fig. 10. Air quality monitors used: a) Temptop 1000s+, b) Temptop M2000.

315 to 400 nm. UVB wavelength ranges between 280 and 315 nm and UVC wavelength ranges between 100 and 280 nm (Fig. 3).

The time required for UV to destroy bacteria or viruses depends on the wavelength of the radiation. UVC radiation requires the least amount of time, as little as a few seconds, but UVA radiation with the same intensity disinfects in minutes or hours.

Unfortunately, the rate of sterilisation or disinfection is directly proportional to the risk to human health. According to international safety guidelines such as EU-Directive-2006-25-EC, UVC radiation is the most harmful, with a maximum exposure time of only a few seconds (depending on wavelength and energy).

To conduct the experiments, as independent variables two ultraviolet LED strips of different wavelengths were selected. One strip was UVA light of 365 nm (14 W/m) and the other was UVC light of 270 nm (10 W/m).

2.2. Bristle material selection

The brush manufacturing company KOTI-Dawson Ltd, UK was requested to provide samples of all the different bristles in which they could make a circular brush with the desired physical characteristics. The materials provided were: Crimped brass, Natural synthetic, Organic Coco, Organic Tampico, Crimped steel, Hand-sanded plastic, Pre sanded plastic. In order to make a valid comparison, the diameter of 0.4 mm was selected for all bristles. A thorough selection was made from all these materials. Initially, biological tests were conducted, followed by microscopic examinations.

The surface of the bristles of any of the chosen inorganic materials, except for pre-sanded plastic ones, is extremely smooth, thus they had to be sanded using a sandblaster. The organic bristles were not sanded, as they were observed to have a naturally rough surface.

To coat the bristles, a solution of water and 2% of TiO_2 powder was created. To improve adherence, it was decided to add 3% of sodium alginate (SA) powder. The solution was stirred and de-bubbled, then the bristles were painted with it. To confirm that SA increased adhesion effectively, microscopic examinations of the bristles were undertaken. Biological tests were then conducted to determine the antiviral impact of the coated bristles.

2.2.1. Microscopic inspection of the coated bristles

As can be observed in Table 1, in general, bristles coated with SA have a more uniform appearance; they contain less gaps uncovered with

the TiO_2 solution. In some cases, such as crimped brass, it is possible to see that with the cover without SA, the TiO_2 is flaking off the bristle.

2.2.2. Antiviral activity trial

The materials were tested for antiviral activity using the same methodology described by Ref. [13]. Briefly, a fixed amount of SARS-CoV-2 was spotted onto each material, left for 10 min and the amount of virus recovered was quantified and compared to a control (no material). Using a cut-off of a 1-log drop in titre (10% of control) to identify anti-viral materials, it was observed that most wire samples with no additional coating had no effect on the stability of SARS-CoV-2 (Fig. 4, labelled as water). The exceptions were the natural Tampico and natural synthetic bristle, for which we did observe a 1-log drop in recovered SARS-CoV-2. However, when materials were coated with sodium alginate (Fig. 4, labelled as SA), the reverse was observed. Almost all materials showed at least a 1-log drop in SARS-CoV-2 titre compared to control, with natural Tampico, pre-sanded plastic and crimped steel showing greater than 1-log drop in SARS-CoV-2 titre compared to control.

3. Prototype description

Two prototypes were designed in accordance with the diagram in Fig. 2. With a motor on the bottom that operates a fan to force contaminated air through a tubular structure housing the mop (cylindrical brush). There, it will be irradiated with UV light to produce the photocatalytic purification reaction. The interior surface of the housing tube is light-reflective to maximise UV ray concentration. The clean air will then be pushed to the outlet by the same fan. The design of this device and its parts is shown in Fig. 5.

The main difference between the two prototypes is that the mop on prototype "A" is not gear-driven to the motor shaft, but on prototype "B" it is. In other words, prototype "A" just pushes air through the mop while it remains stationary, whereas in prototype "B" the mop rotates geared to the motor shaft.

To know the flow characteristics within the device, a CFD simulation was conducted using ANSYS Fluent R2021. As the flow is turbulent different turbulent models are applied and the RNG $k-\epsilon$ is used for the good converging. The converging criteria is set as 10^{-6} for continuity, conservation of momentum and turbulent equations. The governing equations related to the simulations can be found in Ref. [16]. Two cases are conducted including stationary and rotating. Fig. 6a shows the flow simulations when there is not any rotational speed and Fig. 6b demonstrates the flow when 1000 rpm is applied. At the inlet section mass flow rate boundary condition is applied and 0.07 kg/s is given. At the outlet section pressure outlet boundary condition is applied and set as zero (0). Here as can be seen Fig. 6a, when there is not any rotational speed the fluid directly goes the outlet section, and the centre velocity becomes high (average velocity values are identical). But when the rotational speed is applied (Fig. 6b) the air is mixed in different directions and distributed equally all over the mop.

3.1. Prototype construction

With the design depicted in Fig. 5, both prototypes were constructed. Both prototypes were built such that the mops could be easily interchanged. In this way, tests could be carried out with the different materials. Fig. 7a depicts cylindrical mops assembled from ten brush strips of the four chosen materials, from left to right: Brass, Coco, Tampico and Natural synthetic. Each strip brush was covered with the TiO_2 solution previously described. The mops are compatible with both models.

To cause the reaction, LED strips of two different wavelengths were used: 365 nm and 270 nm (Fig. 7b). The tube casing is a sun tunnel rigid extension of 400 mm length and 200 mm of diameter. Two interchangeable reflector tube housings were made for both prototypes, each with a different LED strip attached. The support and assembly parts were

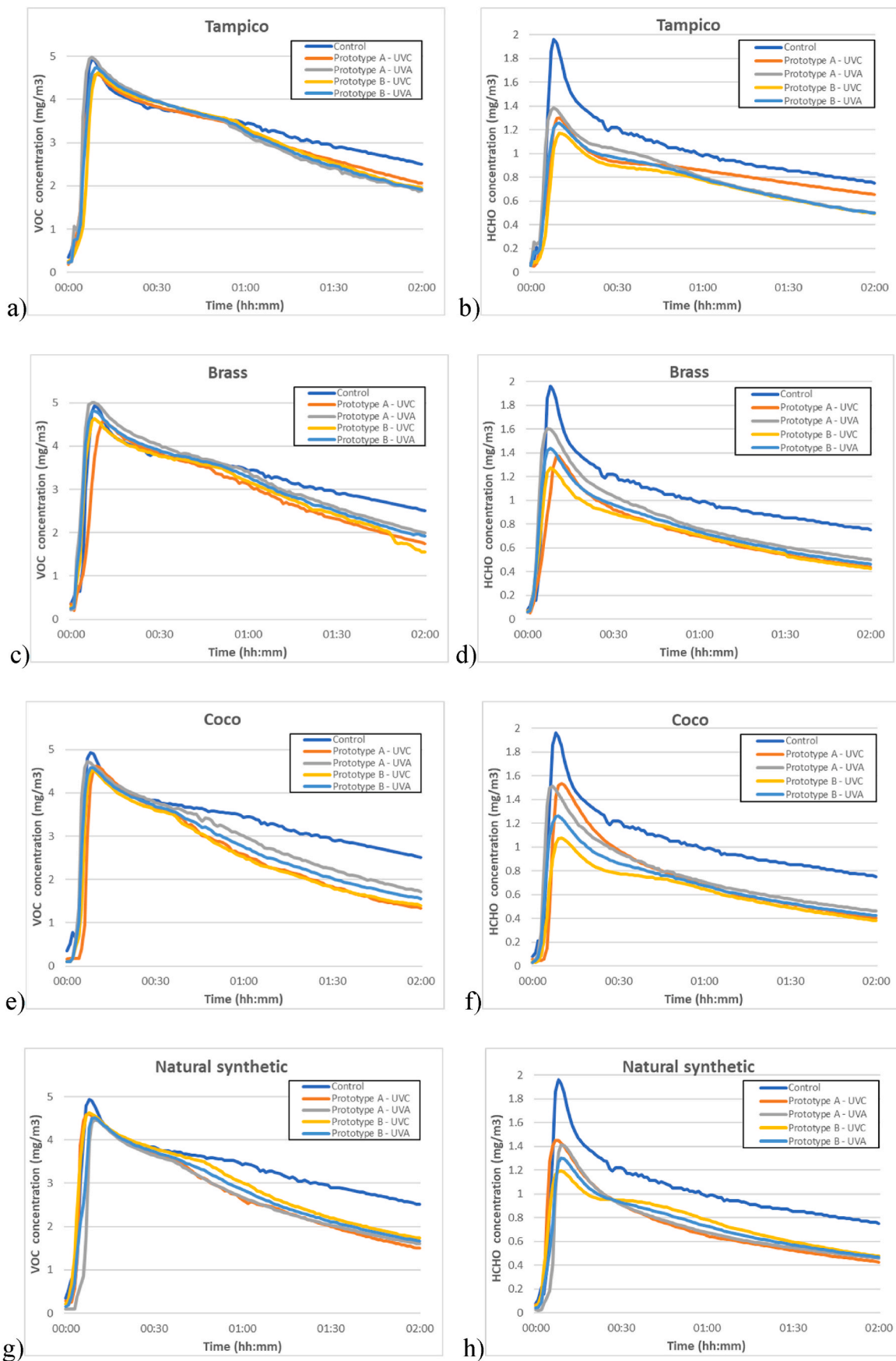


Fig. 11. a) VOC reduction using Tampico. b) HCHO reduction using Tampico. c) VOC reduction using Brass. d) HCHO reduction using Brass. e) VOC reduction using Coco. f) HCHO reduction using Coco. g) VOC reduction using Natural synthetic. h) HCHO reduction using Natural synthetic.

3D-printed in PLA plastic.

Both prototypes utilise a 30W AC motor with a maximum speed of 1300 revolutions per minute. This motor has plastic blades with a 160 mm diameter attached to it (Fig. 7c).

Regarding its construction, prototype B differs from prototype A in that its casing is reinforced by an external structure. Without that structure on prototype B, when the mop spined with the fan blades, a rocking motion was noticed that altered the device's stability and undermined its integrity. The reinforcement consists of four outside 1/4-inch steel supports that hold the lid and reflector tube securely to the base. Fig. 8 depicts the two prototypes with which the tests were conducted. Both have a height of 600 mm and an outside diameter of 200 mm.

4. Experimental procedure

Using the Integrated Environmental Solutions (IES) Virtual Environment software and its Micro Flow function, a simulation was conducted in order to show the way pollution from a point source travels inside a room under experimental settings. The objective of these simulations is simply to visualise the dispersion of pollutants from a certain spot in the room and to demonstrate how the air purifier cleans the air during the tests. A 3D render of the room was exported to the software (Fig. 9a). Two graphs of concentration expressions were generated: particle tracking and concentration map. Fig. 9a and b depict the outcomes of the simulations.

4.1. Test methodology

To analyse the efficacy in real-world circumstances, a purification test was conducted in a real room. The room area is approximately 5 m². The test settings consisted of a controlled 20 °C temperature and 50% relative humidity. To contaminate the air inside the room, 1 ml of methanol was evaporated on a hot plate heated to 80 °C. A Temtop 1000s+ and a Temtop M2000 air quality monitors were utilised to assess the amounts of volatile organic compounds (VOCs) and formaldehyde (HCHO) respectively (Fig. 10). The volume of methanol utilised was adequate to prevent the monitor sensors from becoming overloaded. The prototype was positioned 1 m away to the hot plate to cleanse the room's air. The sensors documented the entire process, including the initial stage, during which the methanol is evaporating until it reaches a peak and secondly, the stage when the pollution concentration decreases. Each testing lasted for 2 h. These tests consist of three factors.

- Motion: Static mop vs Rotating mop (Prototype A vs. Prototype B respectively)
- Light: UVA 365 nm vs UVC 270 nm
- Material: Tampico, Brass, Coco, Natural synthetic

5. Results and discussion

The VOCs and HCHO concentration curves for each test for each of the four MopFan materials are displayed in Fig. 11. In all the graphs, the concentration reaches a maximum peak, which occurs when the methanol evaporates, and air pollution achieves its maximum saturation. In a specific concentration range, the reaction rate for photocatalytic oxidation reduces as the contaminant concentration lowers, since fewer molecules can touch and be absorbed by the MopFan bristles. In addition, each test is compared to the control testing, in which no UV light was applied to the brush, but the fan was activated.

All concentration maximum levels in Fig. 11a are close to the greatest peak in the control test. The degradation thereafter is the same for all variants. On the other hand, in Fig. 11b, it is noted that the highest peak in all situations is greatly lowered. The slopes vary, and prototype B demonstrates the best performance.

The outcomes of the Brass mop tests are depicted in Fig. 11c and d. As hypothesized, given that the substrate was metallic, photocatalysis was achieved effectively. Fig. 11c demonstrates that the concentration of VOCs got below 2 mg/m³ in the best of the tests and is not too far away in the worst. In contrast, its activity to reduce HCHO is more variable, with different types of UV radiation causing differing purification degrees.

Fig. 11e depicts a similar maximum peak to that of the control test; however, after maximum saturation is attained, the VOC decrease curves diverge. UVC radiation appears to be more effective on Coco bristles, however this is not the case with Tampico bristles, which are similarly made of organic material. Fig. 11f depicts a considerable difference between the variations, with the prototype B and UVC light combination being the most effective. Throughout the whole test, the greatest peak is lowered by nearly half and averages 0.4 mg/m³ less than the control.

Fig. 11g demonstrates that the critical points of the curves for Prototypes A and B are quite close, indicating that the UV radiation has little effect on this material. As seen in Fig. 11h, there has been a significant reduction in pollutants.

As both materials are natural organic fibres, it was anticipated that Tampico would react similarly to Coco. However, tests with Tampico were not as successful as those with Coco, perhaps because of Tampico's higher density and lesser porosity. However, its HCHO elimination was comparable to that of the other materials.

Out of all the materials tested, brass was the most costly and difficult material to work with because its bristles were not particularly flexible. When the brass mop was assembled, it ended up being very heavy compared with the mops of the other materials, which caused the revolving prototype (B) to rotate notoriously slower.

After testing the Natural synthetic material, it was discovered that several days after the application of the TiO₂ and SA coating, the bristles of the natural synthetic material lost minute particles of the coating. This renders direct application of this material unfeasible, despite positive test findings.

In every case tested, Prototype B with UVC light appears to be the optimal combo. And after an inspection of all the tests, the one that shows a higher purification rate for both VOCs and HCHO is Prototype B with MopFan made of Coco bristles irradiated by UVC light.

5.1. Photocatalytic mechanism and material influence

One of the essential reasons behind the varying performance of the different MopFan materials lies in their photocatalytic mechanisms. In the presence of UV light, TiO₂ generates electron-hole pairs, which initiate a series of redox reactions that break down VOCs and HCHO into less harmful substances like water, carbon dioxide, and mineral acids. The effectiveness of the photocatalytic process depends on several factors, including the surface properties of the materials, their interaction with UV radiation, and their ability to adsorb and degrade pollutants.

The metallic materials, such as brass, exhibited effective photocatalytic activity due to their conductive nature, which allows for efficient charge separation and transfer, promoting redox reactions on the material's surface. In contrast, organic fibres like Coco and Tampico have different properties. Their naturally rough surfaces provide increased surface area and porosity, which can enhance pollutant adsorption. However, their photocatalytic performance is affected by their composition and structure, with Tampico exhibiting lower efficiency than Coco, possibly due to its higher density and lower porosity.

The synthetic materials showed mixed results, with some losing the TiO₂ and SA coating over time, making their direct application less feasible. The variation in performance among the synthetic materials could be attributed to differences in their physical and chemical properties, such as surface roughness, porosity, and compatibility with the applied coating.

5.2. Role of UV radiation and MopFan prototypes

The role of UV radiation in the photocatalytic process is crucial, as it initiates the electron-hole pair formation in TiO₂. Our results indicate that UVC radiation is more effective in some materials, such as Coco bristles, while having a negligible effect on others like the tested synthetic material. This can be attributed to the differences in UV absorption and penetration in various materials, which affects the generation of electron-hole pairs and the subsequent redox reactions.

Regarding the MopFan prototypes, Prototype B with UVC light consistently showed the best performance in all tested materials. This can be attributed to the enhanced UV exposure due to the rotation mechanism, which ensures a more uniform distribution of UV light on the bristle surface, promoting the formation of more electron-hole pairs and facilitating pollutant degradation.

In summary, the differences in photocatalytic performance among the tested materials can be attributed to their unique physical, chemical, and optical properties, as well as the effectiveness of the MopFan prototypes and UV radiation in promoting photocatalytic reactions. Our findings suggest that the most effective combination for VOCs and HCHO degradation is the use of Prototype B with Coco bristles irradiated by UVC light.

6. Conclusions and future work

The development stages of a sustainable air purifying system based on the concept of a MopFan modified for household use have been given in this paper.

A selection of materials was made from commercially available bristles, including a microscopic inspection of the bristles to find the materials that were best coated with the titanium dioxide (TiO₂) solution. It was determined that the TiO₂ solution works best with 3% sodium alginate (SA). Additionally, trials were conducted to identify the antiviral properties of the coated materials. The following materials were chosen to construct the mops: Tampico, Brass, Coco, and Natural synthetic.

To achieve the objectives of this paper, two MopFan prototypes were designed, constructed, and tested. The prototype "A" with a static mop and the prototype "B" with a spinning mop. Two types of UV ultraviolet light were also tested: 365 nm (UVA) and 270 nm (UVC).

The purpose of the testing was to identify the optimal combination of material, UV light, and mop configuration based on the air purification performance of the MopFan with each kind of material and UV light. The tests were conducted by the University of Nottingham's research team. To achieve realistic settings, the testing was conducted in a real room.

In general, it was found that MopFan decreases the concentration of both volatile organic compounds (VOCs) and formaldehyde (HCHO). Reducing HCHO almost immediately and taking longer to reduce VOCs.

The rotating prototype "B" was shown to give better results. The highest purification was achieved with 270 nm light (UVC).

The results shown that a MopFan rotary mop constructed from Coco fibres and utilising UVC light achieves the best VOC and HCHO purification performance. Within 2 h, this combination lowered HCHO by 50% and VOCs by 23% approximately.

It was found that the LED lights fulfilled the desired purpose in addition to being quite compact. However, as they are surface-mounted LEDs, their luminance is poor. As future work, the ultraviolet illumination might be enhanced. Another possible route for further work would be to scale down the proposed design to build a portable MopFan purifier. If successful, the uses for this purifying technology might expand.

For further studies, it is suggested that a more in-depth analysis of the degradation products at the MopFan outlet be conducted to gain a comprehensive understanding of the air purification process. This analysis should not only include the measurement of VOCs and HCHO concentrations but also investigate the possible presence of by-products

resulting from the photocatalytic reaction. It is also suggested to investigate the possible presence of other air contaminants, such as different gases, particulate matter, or even living organisms, to evaluate the overall performance of the MopFan system. Such an approach would enable a more accurate assessment of the efficiency and safety of the MopFan system, ensuring that no potentially harmful compounds are emitted during the purification process.

Furthermore, these analyses would provide valuable insights into the overall performance of the MopFan system, helping guide the development of improved designs and operational strategies for enhanced air purification.

In addition, a subsequent stage of this study should consider using lower concentrations of air contaminants to simulate a more realistic scenario, allowing for a more accurate representation of real-world conditions. This information would be crucial for refining the MopFan concept and ensuring its practical application in real-world settings, ultimately contributing to the creation of healthier indoor environments.

Funding information

The paper has been submitted as part of an Engineering and Physical Sciences Research Council (EPSRC), UK funded project.

CRediT authorship contribution statement

Emmanuel Tapia-Brito: Writing – review & editing, Writing – original draft, Methodology, Data curation. **James Riffat:** Methodology, Data curation. **Yixin Wang:** Methodology, Data curation. **Yuhao Wang:** Data curation. **Amir M. Ghaemmaghami:** Methodology, Data curation. **Christopher M. Coleman:** Methodology, Data curation. **Mehmet T. Erdinc:** Data curation. **Saffa Riffat:** Writing – review & editing, Supervision, Project administration, Conceptualization.

Declaration of competing interest

The authors declare the following financial interests/personal relationships which may be considered as potential competing interests: Saffa Riffat reports financial support was provided by Engineering and Physical Sciences Research Council.

Data availability

The authors do not have permission to share data.

Acknowledgements

The authors would like to acknowledge the financial support provided for this research by the Engineering and Physical Sciences Research Council (EPSRC), UK Project reference: EP/W010917/1.

References

- [1] J. Saini, M. Dutta, G. Marques, A comprehensive review on indoor air quality monitoring systems for enhanced public health, *Sustainable environment research* 30 (1) (2020) 1–12, <https://doi.org/10.1186/s42834-020-0047-y>.
- [2] J. Kolarik, P. Wargocki, Can a photocatalytic air purifier be used to improve the perceived air quality indoors? *Indoor Air* 20 (3) (2010) 255–262, <https://doi.org/10.1111/j.1600-0668.2010.00650.x>.
- [3] L. Zhong, F. Haghghat, Modeling of by-products from photocatalytic oxidation (PCO) indoor air purifiers: a case study of ethanol, *Build. Environ.* 144 (2018) 427–436, <https://doi.org/10.1016/j.buildenv.2018.08.048>.
- [4] T. Xu, H. Zheng, P. Zhang, Performance of an innovative VUV-PCO purifier with nanoporous TiO₂ film for simultaneous elimination of VOCs and by-product ozone in indoor air, *Build. Environ.* 142 (2018) 379–387, <https://doi.org/10.1016/j.buildenv.2018.06.047>.
- [5] M. Wongaree, et al., Photocatalytic performance of electrospun CNT/TiO sub(2) nanofibers in a simulated air purifier under visible light irradiation, *Environ. Sci. Pollut. Res. Int.* 23 (21) (2016) 21395–21406, <https://doi.org/10.1007/s11356-016-7348-z>.

- [6] L. Zhong, F. Haghighat, Photocatalytic Air Cleaners and Materials Technologies – Abilities and Limitations, vol. 91, Building and environment, 2015, pp. 191–203, <https://doi.org/10.1016/j.buildenv.2015.01.033>.
- [7] M. Kim, et al., Performance of an air purifier using a MnOx/TiO2 catalyst-coated filter for the decomposition of aldehydes, VOCs and ozone: an experimental study in an actual smoking room, Build. Environ. 186 (2020) 1, <https://doi.org/10.1016/j.buildenv.2020.107247>.
- [8] X. Huang, et al., Sterilization system for air purifier by combining ultraviolet light emitting diodes with TiO2, J. Chem. Technol. Biotechnol. 84 (10) (2009) 1437–1440, <https://doi.org/10.1002/jctb.2180>, 1986.
- [9] Y. Sun, et al., Experimental research on photocatalytic oxidation air purification technology applied to aircraft cabins, Build. Environ. 43 (3) (2008) 258–268, <https://doi.org/10.1016/j.buildenv.2006.06.036>.
- [10] Sungwon Kim, et al., Practical scale evaluation of a photocatalytic air purifier equipped with a Titania-zeolite composite bead filter for VOC removal and viral inactivation, Environ. Res. 204 (Pt B) (2022), <https://doi.org/10.1016/j.envres.2021.112036>, 112036–112036.
- [11] A. Pacitto, et al., Effect of Ventilation Strategies and Air Purifiers on the Children’s Exposure to Airborne Particles and Gaseous Pollutants in School Gyms, vol. 712, The Science of the total environment, 2020, <https://doi.org/10.1016/j.scitotenv.2019.135673>, 135673–135673.
- [12] A. Tobisch, et al., Reducing indoor particle exposure using mobile air purifiers—experimental and numerical analysis, AIP Adv. 11 (12) (2021), <https://doi.org/10.1063/5.0064805>, 125114–125114.
- [13] E. Tapia-Brito, et al., Experimental investigation of a MopFan-based photocatalytic air purification device, Future Cities and Environment 8 (1) (2022), <https://doi.org/10.5334/fce.149>.
- [14] S.B. Riffat, H.A. Shehata, Development of a novel mop fan, Int. J. Energy Res. 25 (7) (2001) 601–619.
- [15] International Organization for Standardization, ISO 21348 definitions of solar irradiance spectral categories, Environment 5 (2007) 6–7.
- [16] A. Fluent, 12.0 Theory Guide—1.2 Continuity and Momentum Equations, 2021.